

# MODELING THERMAL FATIGUE IN CPV CELL ASSEMBLIES

Nick Bosco, Timothy J Silverman and Sarah Kurtz  
National Renewable Energy Laboratory, Golden, Colorado, USA

## ABSTRACT

A finite element model has been created to quantify the thermal fatigue damage of the CPV die attach. Simulations are used to compare to results of empirical thermal fatigue equations originally developed for accelerated chamber cycling. While the empirical equations show promise when extrapolated to the lower temperature cycles characteristic of weather-induced temperature changes in the CPV die attach, it is demonstrated that their damage does not accumulate linearly: the damage a particular cycle contributes depends on the preceding cycles. Direct comparison of the FEM with empirical methods and calculation of equivalent times for standard accelerated test sequences were made using CPV cell temperature histories.

## INTRODUCTION

When in service under concentrated direct sunlight, the cell assembly in a concentrating photovoltaic (CPV) module will experience a complex time history of temperature. This history will contain many temperature reversals, or thermal cycles, that will impart stress to the die attach due to a mismatch in coefficient of thermal expansion between the cell and its substrate. With every cycle, inelastic strain energy will be gained by the die attach. The accumulation of this energy will lead to die attach cracking and ultimately to cell failure.

Previous work introduced the rainflow counting algorithm method (RFC) in an attempt to quantify thermal fatigue in the CPV cell assembly's die attach during outdoor exposure [1]. This promised to be a robust method for quickly and simply analyzing service times of many years, however, concessions on the accuracy of the calculation were made. For instance, the thermal fatigue equation employed (Equation 1) was developed for large thermal cycles characteristic of accelerated testing, not for small, quick cycles typical of a CPV cell assembly during service. This equation was also generalized for all materials and applied to the CPV cell assembly geometry, two factors that influence the rate of damage accumulation and that are a departure from the mechanical test samples used for the equation's development. The rate of damage accumulation was also assumed to be linear, meaning that a given cycle does a particular amount of damage independent of how much damage has already been done, thereby giving no consideration to the temperature history of the assembly.

A finite element model (FEM) has been created to quantify the thermal fatigue damage of the CPV die attach. Results

are compared against popular thermal fatigue equations and the previously reported RFC method. The CPV cell assembly temperature history during one month in Golden, Colorado and Phoenix, Arizona are also simulated with the FEM. Comparison of the thermal fatigue damage accumulated during each day of the simulation and through accelerated thermal cycling provides for a direct calculation of the equivalent time of the test sequence.

## MODELING AND APPROACH

### Rainflow Counting

The method of distilling time histories of temperature into discrete thermal cycles via the rainflow counting algorithm has been previously presented and is therefore only briefly reproduced here for clarity [1]. First, a time history of CPV cell temperature is derived from the meteorological data of direct normal irradiance, ambient temperature and wind speed taken at one-minute intervals [2]. The cell temperature history is then distilled into segments of temperature change that are relevant to thermal fatigue using the three-parameter rainflow counting algorithm [3]. Outputs of the rainflow count are temperature change ( $\Delta T$ ), mean temperature ( $T_m$ ) and cycle time ( $t_c$ ) for each cycle. Next, an empirical thermal fatigue equation is used to calculate the relative damage imparted to the die attach with each cycle. In the previous work, the Engelmaier thermal fatigue model was employed [1]. The Engelmaier equation calculates a fatigue life ( $N_f$ , number of cycles to failure) for a specific set of stress conditions [4]. Here, the Engelmaier equation is presented in two forms, one for application on compliant systems ( $E_c$ ) where the maximum stress in the die attach remains below its yield stress throughout cycling:

$$N_f = \frac{1}{2} \left[ \frac{K_c}{\Delta T} \right]^{-1/c} \quad (1)$$

and one for application on stiff systems ( $E_s$ ) where the yield stress of the die attach is exceeded through temperature cycling:

$$N_f = \frac{1}{2} \left[ \frac{K_s}{\Delta T^2} \right]^{-1/c} \quad (2)$$

where the fitting constants  $K_s$  and  $K_c$  are functions of material properties and specimen geometry and the exponent  $c$  depends on the cycle time and mean temperature. Inputs for the Engelmaier equation are therefore the three outputs of the rainflow algorithm. In

the current paper, the Coffin-Manson model is also presented [5]:

$$N_f = K_{CM} \Delta T^{-2} f^{1/3} \exp\left(\frac{E_a}{kT}\right) \quad (3)$$

This equation, demonstrated by experiment to be valid for ceramic and plastic packages attached with SnPb solders, computes  $N_f$  for a unique thermal cycle characterized by its  $\Delta T$ , cycle frequency ( $f$ ) and an Arrhenius dependence on the maximum cycle temperature ( $T_{max}$ ) where an activation energy of  $E_a = 0.12$  eV is typically used for SnPb solder, and  $k$  is Boltzmann's constant [6, 7]. The fitting parameter,  $K_{CM}$ , cancels out for relative comparisons. This empirical relationship is included for comparison to the results of the Engelman equations and FEM simulations.

Following similar methods of quantifying thermal fatigue damage during the service life of electronic components, the Palmgren-Miner hypothesis is used in this analysis [3]. The Palmgren-Miner hypothesis states that die attach damage,  $D$ , is considered to be linearly proportional to the ratio of the number of cycles completed at a specific set of stress conditions ( $i$ ),  $n_i$ , to the total number of cycles that would result in failure for those same conditions,  $N_{f,i}$ :

$$D_i = \frac{n_i}{N_{f,i}} \quad (4)$$

Because every cycle computed using the rainflow count represents a unique stress condition ( $n=1$  for all  $i$ ), the damage accumulated through the temperature history of interest is calculated by summing the inverse of the relevant fatigue equation over every cycle in the time history.

$$D = \sum_i \frac{1}{N_{f,i}} \quad (5)$$

### Finite Element Analysis

A 3D model of a generic CPV cell assembly was generated using COMSOL. The assembly consists of a  $1 \text{ cm}^2 \times 100 \text{ }\mu\text{m}$  Ge die attached to a direct-bond copper (DBC) substrate via  $25 \text{ }\mu\text{m}$  of eutectic SnPb solder. The DBC is modeled as a  $2.3 \times 2.7 \text{ cm}$  layered structure composed of a  $250 \text{ }\mu\text{m}$  thick layer of  $\text{Al}_2\text{O}_3$  sandwiched by two  $200 \text{ }\mu\text{m}$  layers of Cu. The rate-dependent creep behavior and the time-independent plasticity of the solder is characterized by Anand's model [8]. This constitutive model represents the two different creep mechanisms of Sn-containing solders: grain boundary sliding or dislocation glide (low stress and high temperature) and dislocation climb (high stress and low temperature).

Darveaux's approach is taken to evaluate the solder's lifetime. Derived from the Paris power law of fatigue crack growth, the Darveaux approach considers the inelastic strain energy density as a damage indicator [9].

Accordingly, both crack initiation and growth are functions of the average inelastic strain energy density (plastic work) accumulated per loading cycle. In the current study, the two phases of failure are not differentiated, therefore only the total plastic work is considered as the metric for damage.

### SIMULATIONS

Three types of thermal cycle, corresponding to the thermal cycles in the CPV design qualification test (IEC 62108) and shown in Table 1 (including the dwell time  $t_d$ ), were simulated. To determine the applicability of the various methods to temperature cycles typical of service conditions, the sensitivity of the FEM and the empirical equations to the cycle parameters ( $\Delta T$ ,  $T_m$ , and  $t_c$ ) was explored using the ranges in Table 2.

	TCA-1	TCA-2	TCA-3
$T_{max}$ (°C)	85	110	65
$T_{min}$ (°C)	-40	-40	-40
$t_c$ (min)	100	100	100
$t_d$ (min)	10	10	10

**Table 1. Simulated thermal cycles corresponding to options in IEC 62108**

varied parameter:	temp change	mean temp	cycle time
$\Delta T$ (°C)	5-50	25	30
$T_m$ (°C)	35	5-75	35
$t_c$ (min)	16	16	4-32

**Table 2. Range of parameters explored using FEM**

To address the Palmgren-Miner hypothesis of linear damage accumulation, the effect of temperature history was studied. This study was conducted by simulating a repetition of 50 cycles ( $\Delta T = 25^\circ\text{C}$ ,  $T_m = 35^\circ\text{C}$ ,  $t_c = 16$  min), then changing the mean temperature and continuing the simulation for an additional 50 cycles. Fourteen trials were simulated, representing changes in mean temperature,  $\Delta T_m$ , from  $-35^\circ\text{C}$  to  $35^\circ\text{C}$  in  $5^\circ\text{C}$  increments.

Finally, the CPV cell temperatures for one month experienced in Golden, Colorado and Phoenix, Arizona were derived from one-minute weather data and used in FEM simulations.

Due in part to the presence of strain hardening in the FEM, repeated cycles can each contribute different amounts of work. For all temperature cycle simulations, a minimum of 50 cycles was repeated and the damage reported is all inelastic strain energy density accumulated from the three out-of-plane stress components in the die

attach for the last cycle. For the weather simulations, each month was run five consecutive times and the results of the fifth repetition reported.

## RESULTS AND ANALYSIS

### Thermal Cycling

The inelastic strain energy density (damage) accumulated during a single cycle of each of the three *TCA* types is presented in Fig. 1, normalized to unity for the most damaging cycle. Also shown in the figure are the fits of the two Engelmaier equations (*Ec* and *Es*) along with the result of the Coffin-Manson (C-M) model for the same cycles. The Engelmaier fits are denoted *TCA* to represent that their constants were adjusted to match the ratio of damage calculated from the FEM simulations of these *TCA* cycles ( $K_{c,TCA}=35$  and  $K_{s,TCA}=2000$ ). The Coffin-Manson model fit the FEM well using the reported activation energy, as did the two fitted Engelmaier equations.

The FEM simulations of the twenty-nine weather-type cycles are presented in three plots according to the varied parameter, Figs. 2–4. These results were used to provide a corresponding *weather* fit of the Engelmaier and Coffin-Manson equations, which are also included in the figures, and normalized to the most damaging cycle as determined by the FEM simulation. In this case, adjustment of the *Ec* constant ( $K_{c,weather}=5.35e6$ ) was required to achieve a satisfactory fit to the FEM simulations and no fit of the *Es* equation was possible, so it is omitted. Similarly, adjustment of the Coffin-Manson's activation energy was also required ( $E_{a,weather}=0.9$  eV) which corresponds closely to the activation energy, determined by experiment, for the constitutive model used in the finite element simulation ( $E_{a,FEM}=0.93$  eV). While the *Ec* equation does appear capable of fitting cycles in both the *TCA* and *weather* regimes, the fitting constant is not intended to be adjusted according to cycle characteristics.

The results of the series of simulations to explore the hypothesis of linear damage accumulation are presented in Fig. 5. Results are presented as a ratio (closed symbols) of damage during the first cycle to damage during the last cycle after the mean temperature shift, and as an absolute change in damage (open symbols). A ratio of unity would signify a linear relationship and is only present at zero change in mean temperature. The asymmetric response of damage ratio around mean temperature change is an artifact of the results being compounded with the effects of mean temperature: at higher temperatures the kinetics for stress relaxation become more favorable. The symmetrical response of absolute damage illustrates that the higher temperature cycles are more damaging. Despite the previous results that show promise in reconciling the FEM simulations and empirical thermal fatigue models, this clear nonlinearity will prevent the application of an empirical model that does not also include some consideration of temperature history.

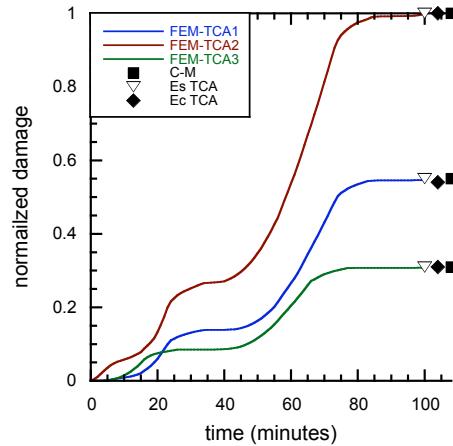


Figure 1. FEM damage accumulated through the *TCA* thermal cycles and corresponding empirical fits.

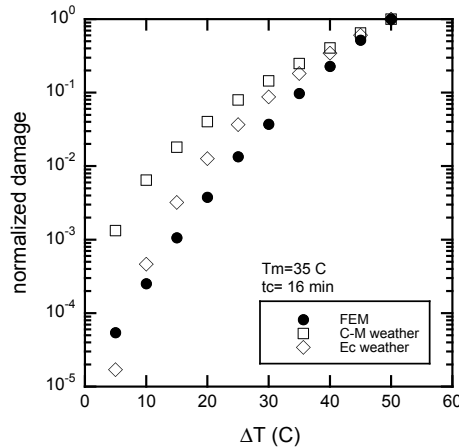


Figure 2. Relative comparison of FEM and empirical fits sensitivity to magnitude of cycle temperature change.

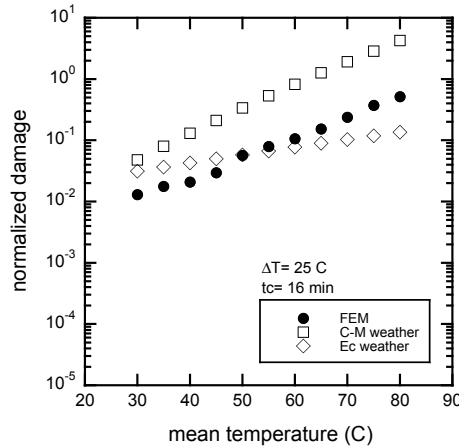
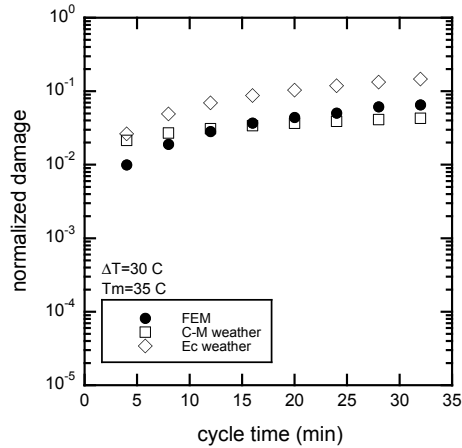
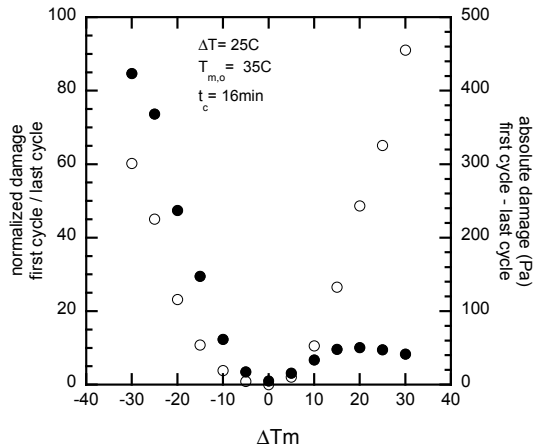


Figure 3. Relative comparison of FEM and empirical fits sensitivity to mean cycle temperature.



**Figure 4. Relative comparison of FEM and empirical fits sensitivity to cycle time.**



**Figure 5. Ratio of damage (closed symbols) of the first to last cycle following a shift in mean cycle temperature. The same results are reported in terms of absolute damage (open symbols).**

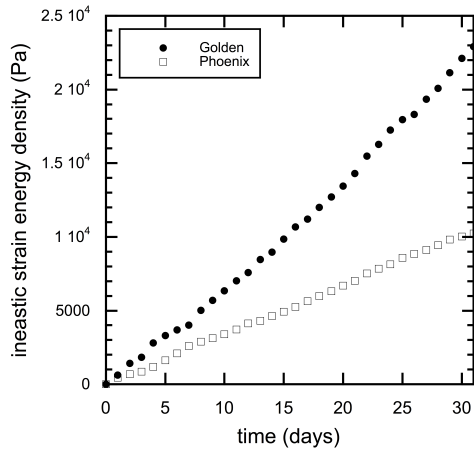


**Figure 6. Inelastic strain energy density (FEM) accumulated for Golden and Phoenix.**

## The Weather

The simulations of each month in Golden, Colorado and Phoenix, Arizona are first summarized by the accumulated inelastic strain energy density (damage) by day in Fig. 6. Over the course of these months, the die attach of an identical assembly in Phoenix would accumulate roughly 45% of the damage accumulated in Golden. Three days in Golden are presented separately in Figs. 7–9. Each plot contains the modeled cell temperature and its associated inelastic strain energy density (damage) accumulated throughout the day. The relative damage calculated through the FEM simulation and the RFC method using both the C-M and Ec weather regime fits for the thermal fatigue equation are also included. First, July 29, a very damaging, partly cloudy day is presented and used for the normalization, Fig. 7. On this day, several long periods of clouding occur. Next, July 10, a sunny day with no clouds is presented where, according to the FEM, roughly half the damage is accumulated compared to July 29, Fig. 8. While both the C-M and Ec results agree with the FEM result that the sunny day causes less damage, both of the empirical damage equations substantially underestimate the magnitude of the difference.

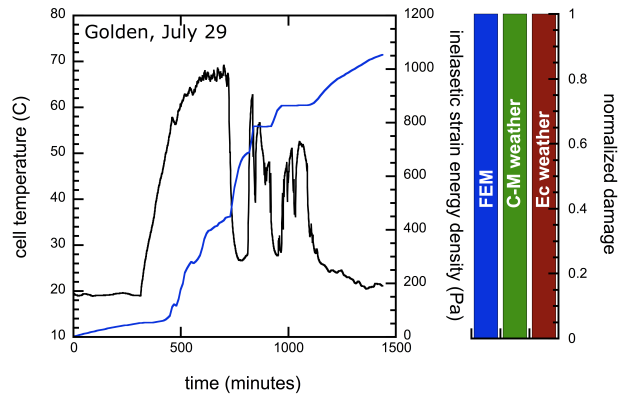


**Figure 7. Golden July 29: Modeled cell temperature, accumulated inelastic strain energy density (FEM) and RFC method results.**

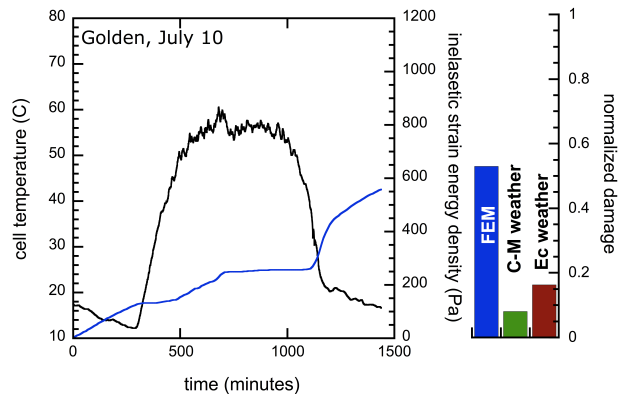


**Figure 8. Golden July 10: Modeled cell temperature, accumulated inelastic strain energy density (FEM) and RFC method results.**

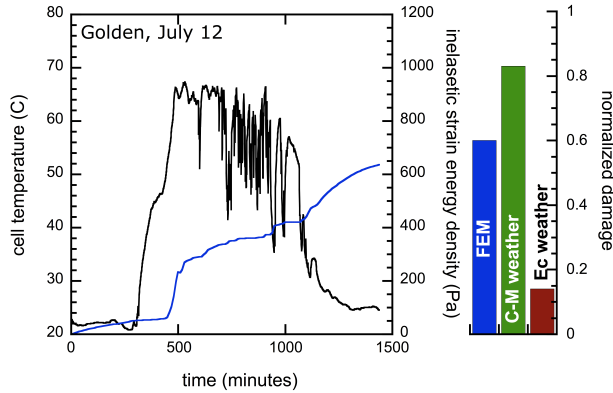


**Figure 9. Golden July 12: Modeled cell temperature, accumulated inelastic strain energy density (FEM) and RFC method results.**

Finally, another partly cloudy day is presented, July 12, which contains many short periods of clouding, Fig. 9. In this case, according to the FEM, the simulated damage is only slightly larger than on the sunny day. The C-M model overestimates the relative damage of July 12 while the Ec model does not significantly change with respect to July 10, the sunny day.

Two similar figures for days in Phoenix are presented in Figs. 10–11. The most damaging day of the month, according to FEM results, is August 22 and is presented in Fig. 10. This day causes damage very comparable to the similarly cloudless day in Golden, July 10. The last day presented, August 5, contains many short periods of clouding, similar to July 12 in Golden, but causing ~12% less damage, Fig. 11. The simulated cell temperature and accumulated damage for August 22 are superimposed (light grey and light blue curves) to illustrate the similar temperature profiles of these days, save the effect of short period clouding on Aug 5.

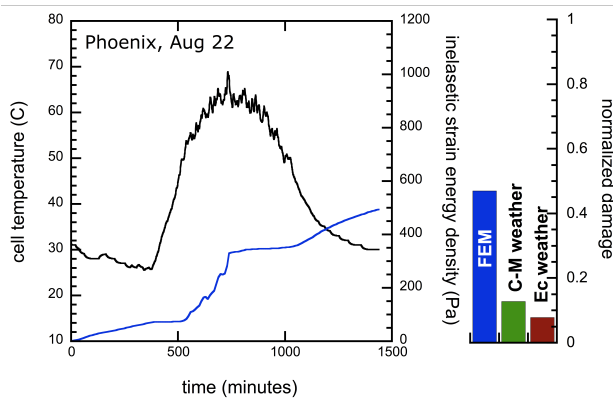


**Figure 10. Phoenix, AZ August 22: Modeled cell temperature, accumulated inelastic strain energy density (FEM) and rainflow results.**

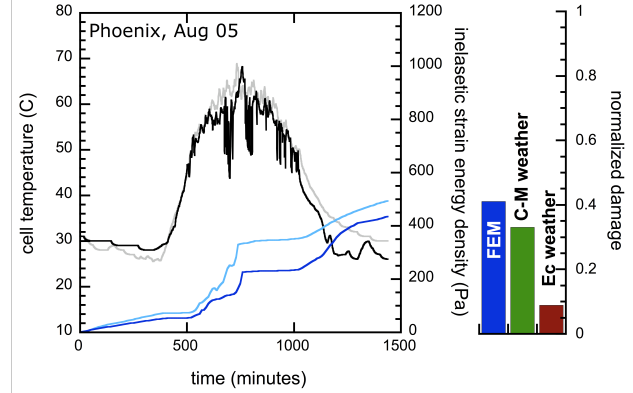


**Figure 11. Phoenix August 5: Modeled cell temperature, accumulated inelastic strain energy density (FEM) and RFC method results.**

### Equivalent Time

The preceding simulation results and analysis provide an estimate of equivalent time for standard accelerated testing sequences, Table 3. The values in this table are produced by relating the energy accumulated through the TCA cycles simulated, Fig. 1, to the energy accumulated during each characteristic day or month. Therefore the values of equivalent time represent consecutive characteristic days or months. As per IEC 62108, the number of cycles considered for each test are 1000, 500 and 2000 for the TCA1, 2 and 3 sequences, respectively.

	equivalent time (years)				
	Golden July 10	Golden July 29	Golden July	Phoenix Aug 22	Phoenix Aug
TCA1	15	9	13	20	29
TCA2	14	8.5	12	18	27
TCA3	18	11	15	23	34

**Table 3. Equivalent times for the standard IEC 62108 testing sequences.**

### DISCUSSION

The FEM simulations are easily fit by the three popular empirical equations considered in this study. Both forms of the Engelmaier equation required fitting in the TCA regime because they include a material- and specimen-dependent fitting constant. The Coffin-Manson equation required no fitting in the TCA regime when used with the activation energy reported from the literature for SnPb solder. In the weather regime, only the compliant form of the Engelmaier equation provides a satisfactory fit to the FEM simulations. This result is consistent with the CPV assembly acting as a compliant part ( $\sigma_{max} < \sigma_{yield}$ ) for small cycles, however a large adjustment of the fitting constant was required to achieve this fit. Considering that the form of the constant is not dependent on cycle character, this may be a fortuitous result. The Coffin-Manson equation is also capable of providing a fit within the weather regime. In this case, the best fit is achieved with an activation energy very similar to the one employed in the constitutive

equations of the FEM, suggesting a more physical meaning.

The period and duration of clouding and the mean temperature appear to have the largest influence on the amount of damage accumulated during a day. The above results suggest that fewer, longer-period clouds are more damaging than many short-period clouds. This effect may be compounded by the lower temperature achieved during a longer shading period, and by the length of time the solder is given to relieve the stress of the associated temperature change by inelastic strain, thereby accumulating energy. The short shading events do not provide as large a driving force (temperature change) nor do they allow adequate time for stress relief through inelastic strain. These effects are clearly illustrated in Fig. 11, where short periods of clouding are shown not to contribute much additional damage over a similar temperature day without clouds. The inaccuracy of the empirical models may primarily be attributed to the nonlinear accumulation of energy as illustrated by the FEM analysis, Fig. 5.

### CONCLUSIONS

A FEM was created to quantify the thermal fatigue damage accumulated in the CPV cell assembly die attach through thermal cycling and outdoor exposure. First, results are compared to three popular thermal fatigue equations and indicate positive correlations when evaluating 29 types of small thermal cycles motivated by weather-induced temperature changes. The accumulation of damage, however, is shown to be nonlinear for adding adjacent cycles of different character. This observation disproves the Palmgren-Miner hypothesis, which is extensively used in the literature for similar methods of quantifying thermal fatigue. Considering the trends in damage with cycle parameter elucidated from the FEM, characteristic days from Golden, Colorado and Phoenix, Arizona were analyzed. It was observed that periods of long clouding contribute more damage than shorter ones. For the months analyzed, these types of days were prevalent in Golden and absent in Phoenix. The analysis of the TCA cycles and weather data provided for an estimate on the equivalent time for the IEC 62108 thermal cycling sequences. The range in equivalent times varied between 8.5 and 18 years for the most damaging day considered in Golden and Phoenix, respectively.

While the accuracy of the FEM is desirable, software and hardware costs and computing times are prohibitive. Alternative approaches based on the direct computation of damage from a given sequence of temperatures are much simpler to implement. But the empirical damage equations investigated here are inappropriate for computing damage due to weather. A new model is needed that properly computes damage done by small temperature cycles and that accounts for the history dependence of damage accumulation without the cost and complexity of the FEM. The result will be an easily implemented method to calculate both the relative thermal fatigue damage

accumulated between deployment locations and the equivalent times of exposure for those locations through thermal cycling. Methods to explore the consequence in reliability on cell assembly materials and geometry are also required.

### REFERENCES

- [1] N. Bosco and S. Kurtz, "Quantifying the Thermal Fatigue of CPV Modules," *AIP Conference Proceedings*, vol. 1277, pp. 225-228, 2010.
- [2] D. L. King, *et al.*, "Photovoltaic array performance model," Sandia National Laboratories SAND2004-3535, 2004.
- [3] A. Ramakrishnan and M. G. Pecht, "A life consumption monitoring methodology for electronic systems," *Components and Packaging Technologies, IEEE Transactions on*, vol. 26, pp. 625-634, 2003.
- [4] W. Engelmaier, "Generic reliability figures of merit design tools for surface mount solder attachments," *Components, Hybrids, and Manufacturing Technology, IEEE Transactions on*, vol. 16, pp. 103-112, 1993.
- [5] K. C. Norris and A. H. Landzberg, "Reliability of Controlled Collapse Interconnections," *IBM Journal of Research and Development*, vol. 13, pp. 266-271, 1969.
- [6] A. E. Perkins and S. K. Sitaraman, *Solder Joint Reliability Prediction for Multiple Environments*. New York: Springer, 2009.
- [7] H. Cui, "Accelerated temperature cycle test and Coffin-Manson model for electronic packaging," in *Reliability and Maintainability Symposium, 2005. Proceedings. Annual, 2005*, pp. 556-560.
- [8] G. Z. Wang, *et al.*, "Applying Anand Model to Represent the Viscoplastic Deformation Behavior of Solder Alloys," *ASME Journal of Electronic Packaging*, vol. 123, pp. 247-253, 2001.
- [9] R. Darveaux, "Effect of simulation methodology on solder joint crack growth correlation," in *Electronic Components and Technology Conference, 2000. 2000 Proceedings. 50th*, 2000, pp. 1048-1058.